nature communications

Article

https://doi.org/10.1038/s41467-025-57619-7

Selective transformation of propargylic ester towards tunable polymerization pathways

Received: 19 September 2024

Accepted: 26 February 2025

Published online: 04 March 2025

Check for updates

Haiyan Hu[1,2], Xuelun Duan[1,2], Ming Li[1,2], Wangze Song[1], Haotian Shi[1], Guofeng Wang[1] & Nan Zheng[1]

Divergent synthesis of numerous complex molecules has emerged as a promising strategy as it allows the access to structurally distinct products from identical starting materials. However, selective transformation of the same monomer into diverse polymers by modulating the polymerization conditions remains a synthetic challenge. In this work, we report the design of propargylic ester, which can be selectively transformed into polyimidate, polyimine, or polyamidine through distinct polymerization pathways. By modulating polymerization conditions, either ester migrating or ester leaving can be selectively manipulated with the formation of different nitrogen-containing intermediates including imine, ketenimine, and alkylidene ketenimine. Three types of polymers could be exclusively obtained using one set of monomer combination containing propargylic ester and sulfonyl azide. In this work, the tunable ester leaving or migrating ability for propargylic ester allows it as a variable synthon monomer, which can facilitate varied transformations towards structure-diverse polymers.

Divergent synthesis of complex molecules from the essentially identical starting materials has attracted enormous attentions in chemistry area because it can improve both the efficiency of chemical synthesis and the versatility of the products[1–3]. With the advancement of divergent synthesis in organic chemistry, diversified polymerization is highly desirable but challenging in polymer and materials science to construct polymers endowed with tailored properties[4]. Recently, several strategies, exemplified by multicomponent polymerizations (MCPs), have been raised to exponentially enrich polymer structures with the combination of at least three monomers[5,6]. Complementarily, the selective transformation of one single monomer to versatile polymers through tunable polymerization pathways is also showing great potential in producing structure-diverse polymers. Unlike traditional polymerization methods and the recently developed MCP strategy, variable and tunable polymerizations offer an alternative and unique approach to generating distinct categories of polymers bearing variable interunit linkage structures.

In organic synthesis, it is not uncommon to employ specific chemical structures as synthons to generate versatile molecules under various conditions[7–9]. However, it has been rarely explored as specific monomer to perform variable polymerizations, despite the significant advantages in flexibly constructing categories of polymers. The reason is straightforward as it is much more difficult to selectively transform a synthon to versatile polymers than to different small molecules due to the constraints imposed by the macromolecular framework[10]. In organic synthesis, moderate reactivity and selectivity are tolerable, as pure compounds can be obtained through subsequent purification techniques. However, polymerization generally requires more tough and strict control over both reactivity and selectivity due to the fact that even minor side reactions can inevitably lead to the formation of difficult-to-remove structural defects within the polymer chains[11]. Therefore, we wonder whether it is possible to design a specific monomer structure, which can be efficiently transformed into different types of polymers in a highly selective manner.

One strategy to achieve tunable polymerizations is to afford similar yet distinct intermediates by selective transformation of the single monomer. Imine, ketenimine (also can be called as aza-cumulated-diene or aza-[2]cumulene), and alkylidene ketenimine

[1]School of Chemical Engineering, Dalian University of Technology, Dalian, Liaoning, China. [2]These authors contributed equally: Haiyan Hu, Xuelun Duan, Ming Li. e-mail: nzheng@dlut.edu.cn

(also can be called as aza-[3]cumulene) are the crucial nitrogen-containing electrophilic intermediates. Ketenimines and alkylidene ketenimines bearing the cumulated double bonds possess desired electron-rich properties and chemical reactivity due to the extended π-bonds[12,13]. Besides alkylidene ketenimines as very limited example reported by our group[14], both imines, and ketenimines have been widely applied in constructing polymers. For example, polyimines were usually synthesized by Schiff base condensation of amines and carbonyl groups serving as the crucial linkages in COF and MOF[15–17]. Choi, Hu, Tang, and our groups have developed a series of MCPs involving ketenimine intermediates[18–22]. Recently, our group disclosed an electronic effect control synthesis of poly(triazole-*alt*-*Z*-acrylamides) via alkylidene ketenimines[14]. Most recently, Zhu reported the unique preparation of all carbon unsaturated backbone polymers from propargylic esters involving long cumulene intermediates[23–25]. Inspired by the previous findings, we wonder whether propargylic ester could be selectively transformed into different nitrogen-containing intermediates by reacting with suitable nitrogen source, thereby realizing the tunable polymerization pathways and affording structure-diverse polymers.

In this work, propargylic ester is disclosed to efficiently prepare three kinds of polymers (polyimidates, polyimines, and polyamidines) through different polymerization pathways under varied conditions (Fig. 1). Owing to the specific structure of propargylic ester, ester group shows dual characters as both migrating and leaving. The ester migrating was mainly relied on the weak nucleophilicity of carbonyl group while its leaving property was mainly based on the C-O bond breakage[26]. Once upon the ester migration, either 1,3-ester migrating (also as a type of [3,3]-sigmatropic rearrangement) or 1,2-ester migrating (also as a type of [2,3]-sigmatropic rearrangement) would occur under different conditions. Polyimidates could be accessed as the 1,3-ester migrating products following the pathway A including triazole formation, N_2 exclusion induced ketenimine generation, and the 1,3-ester migration (Pathway A)[27]. On the other hand, when copper(I) thiophene-2-carboxylate (CuTC) and Rh(II) were used as catalysts, an α-imino Rh-carbene intermediate could be formed via the ring opening of sulfonyl triazole and N_2 releasing, resulting in the 1,2-ester migrating (Pathway B)[28–30]. Hence, polyimines as the 1,2-ester migrating products could be afforded. Additionally, ester could also leave rather than migrate with the existing of nucleophiles, either ketenimine or high-reactive alkylidene ketenimine could be possibly generated as shown in pathway C, affording polyamidines as the MCP products (with amino-based nucleophiles). In this work, propargylic ester, as a variable synthon monomer (VSM), has been successfully utilized to generate different intermediates with tunable polymerization pathways. Such strategy also provided a valuable insight in the design of particular monomers towards diverse polymers.

Results and discussion

Substrate scope and structure characterization for VSM-induced polymerizations

To facilitate the controlled ester migrating or leaving, propargylic benzoates bearing electro-donating ester groups were designed as the VSM. Sulfonyl azide (SA) was selected as the nitrogen source to react with propargylic benzoates, yielding different nitrogen-containing intermediates and polymers under varied conditions (Fig. 2). In pathway A, Cu(I) (both organic or inorganic Cu(I) except for CuTC) was selected as the catalyst, affording polyimidate following the routes of cycloaddition, N_2 exclusion induced ketenimine generation, and the 1,3-ester migration. Upon the change of catalytic system, the ester migration site could vary as indicated in pathway B. CuTC is a unique Cu(I) catalyst containing sulfur, five-membered aromatic heterocycle, and carboxylate. It can dramatically change the reaction between terminal alkyne and sulfonyl azide to give the single 1-sulfonyl triazole in exclusive selectivity, for the reason that CuTC can stabilize 5-Cu(I)-1,2,3-triazole and disfavor the conversion to the ketenimine[28]. Therefore, the N_2 exclusion-induced ketenimine generation pathway was inhibited and the stable sulfonyl triazole formed. Upon the subsequent catalyzed by Rh(II), α-imino Rh carbene could be generated with the Rh(II) assisted N_2 exclusion. Therefore, ester could migrate to Rh carbene site under the bimetallic relay catalysis by CuTC and Rh(II), affording polyimine as the 1,2-ester migrating product. In pathway C, ester could leave by the addition of competitive nucleophile such as *N*-methylaniline (**Nu1**), with the formation of polyamidine under the Cu(I) catalysis. To render the polymer names more concise, the products were designated as P(x-y-A), P(x-y-B), and P(x-y-z-C) based on the

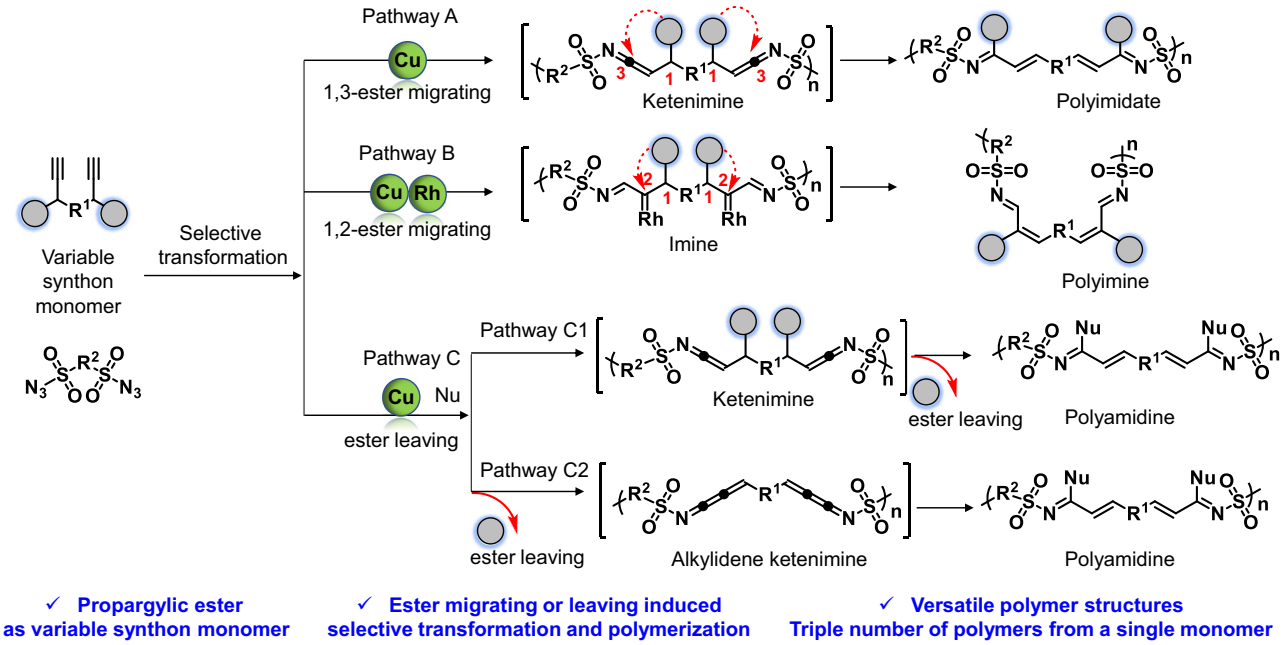

Fig. 1 | Polymerization pathways. Three polymerization pathways starting from propargylic esters as the variable synthon monomers for the facile preparation of polyimidates, polyimines, and polyamidines.

https://doi.org/10.1038/s41467-025-57619-7

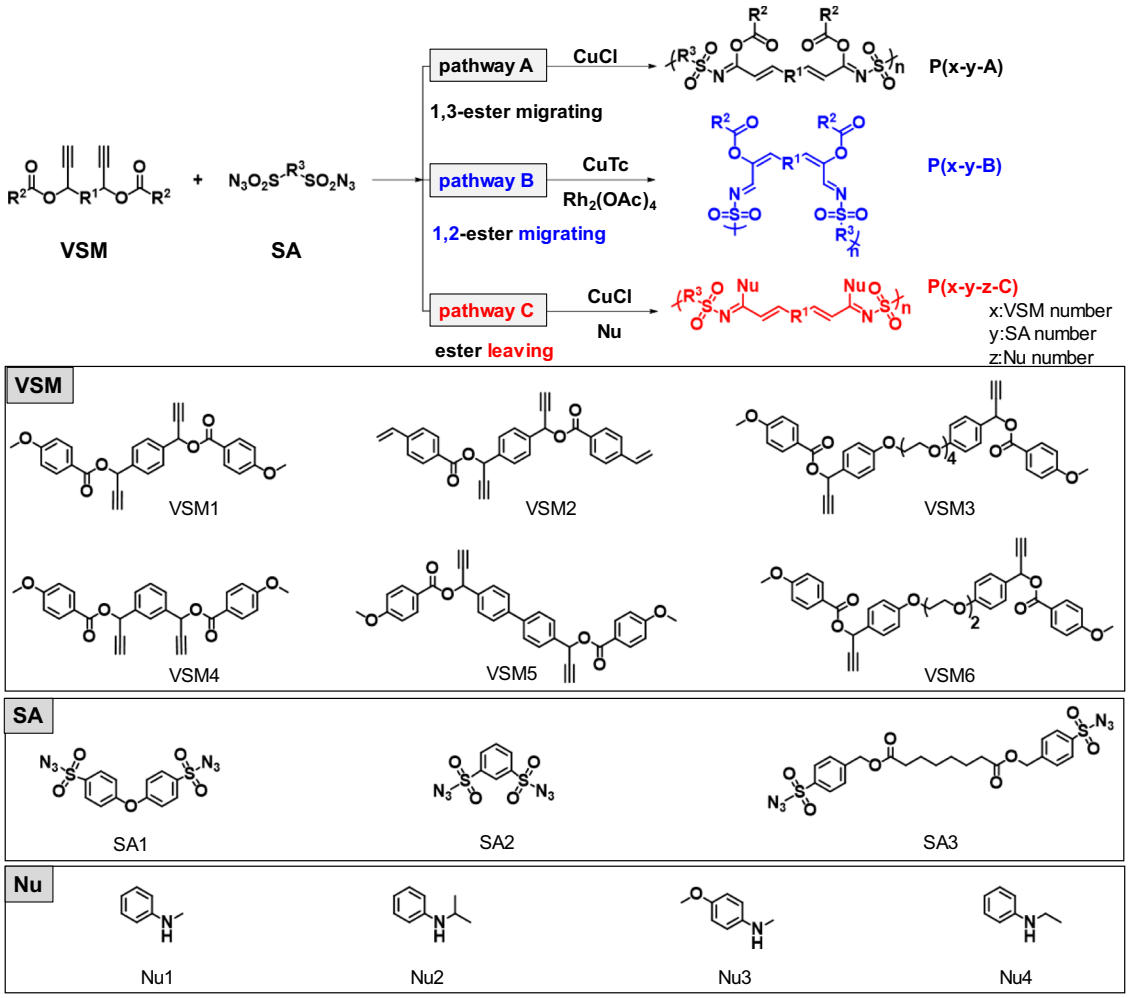

Fig. 2 | Monomer scope. VSM-induced three types of polymerizations and the monomer substrates.

monomer combinations and polymerization pathways (Fig. 2, x meant VSM number, y meant SA number, and z meant Nu number).

To explore the monomer scope and investigate whether triple number of polymers could be selectively prepared from the single monomer combination, 6 propargylic benzoates-based VSMs (**VSM1-VSM6**), 3 SAs (**SA1-SA3**) and 4 Nus (**Nu1-Nu4**) were designed and prepared (Fig. 2). All the monomers (except for the commercially available compounds) and polymers were carefully characterized by NMR spectra and GPC (monomers: Supplementary Figs. 19–34; polymers: Supplementary Figs. 35–75; GPC: Supplementary Figs. 102–103). The monomer information and polymerization results are summarized in Table 1. It was delighted to find that 24 polymers (entries 1-24 in Table 1) could be obtained within 8 kinds of monomer combinations in high yields (up to 97%) and molecular weights (M_ns) (up to 20,000 g/mol). The polydispersity index ($Đ$) of most of the obtained polymers was about 1.2-1.8 since the post-polymerization purification would reduce the $Đ$ value to some extent. Various functional groups including the OMe, vinyl, biphenyl, and multi-ether groups in VSMs could be well tolerated in all the polymerizations. All the polymers had excellent solubility in polar solvents like DMSO and DMF. Detailed solubility and color information of all the polymers were summarized in Supplementary Table 9.

The polymerization results were firstly analyzed by comparing the yields and M_ns between ester migrating pathways (A and B) and leaving pathway (C). It can be noted that most of P(x-y-z-C) (products from pathway C) exhibited slightly higher M_ns (>13,000 g/mol) than the products obtained from pathway A or B (< 11000 g/mol), which could be attributed to the feature of Nus as bases. Amino Nu could act as the base to accelerate the cycloaddition and N_2 exclusion process, which ultimately improved the reactivity of the polymerization and increased the M_ns. From the steric effect aspect, bulky and steric ester groups on the side chains would also slightly affect the M_ns of obtained polymers in pathways A and B because the migrating process could possibly interfere the cycloaddition reactivity at the late-stage of polymerization. However, when **VSM3** or **VSM6** containing ethers were selected as the monomers, the related polymers owned significantly enhanced M_ns (>12,000 g/mol) due to the improved solubility. Polymers from **VSM3** bearing 4 ether groups showed higher M_ns (15,500–20,000 g/mol) than those from **VSM6** bearing 2 ether groups (11,600–16,700 g/mol), supplementarily demonstrating the crucial roles of solubility. From the SA aspect, using both **SA1** and **SA3** could afford the polymers with similar M_ns by the same polymerization pathways (Table 1, entries 1 and 22; entries 2 and 23; entries 3 and 24). However, polymers from **SA2** exhibited reduced M_n in pathways A and C due to the *meta*-substitution induced steric hindrance effect (Table 1, entries 19&21). However, in pathway B, M_n did not notably vary with the change of SA (Table 1, entry 20). It was possibly because the side chain in P(x-y-B) was substituted on the less steric alkene groups, while in pathway A or C, the side chain was substituted on imine adjacent to large steric sulfonyl group.

Polymers from 1,3-migrating or 1,2-migrating pathways also showed different M_ns. It can be noticed that P(x-y-A) derived from pathway A, generally exhibited relatively higher M_ns than P(x-y-B) from pathway B. This discrepancy may be attributed to the introduction of

https://doi.org/10.1038/s41467-025-57619-7

Table 1 | Summary of polymerization results under different pathways.[a]

Entry	Monomer combination		Polymer	Yield/% [b]	M_n/(g/mol) [c]	$Đ$ [c]
	VSM	SA				
1	VSM1	SA1	P(1-1-A)	85	10500	1.18
2			P(1-1-B)	90	7900	1.36
3			P(1-1-1-C)	90	13800	1.17
4	VSM2	SA1	P(2-1-A)	82	11500	1.34
5			P(2-1-B)	80	6900	1.18
6			P(2-1-1-C)	92	13000	1.45
7	VSM3	SA1	P(3-1-A)	85	15500	1.62
8			P(3-1-B)	85	20000	1.47
9			P(3-1-1-C)	97	17600	1.73
10	VSM4	SA1	P(4-1-A)	90	8700	1.10
11			P(4-1-B)	78	4600	1.02
12			P(4-1-1-C)	94	11000	1.21
13	VSM5	SA1	P(5-1-A)	88	10500	1.46
14			P(5-1-B)	86	6300	1.20
15			P(5-1-1-C)	96	14000	1.53
16	VSM6	SA1	P(6-1-A)	86	11900	1.41
17			P(6-1-B)	84	11600	1.44
18			P(6-1-1-C)	87	16700	1.42
19	VSM1	SA2	P(1-2-A)	89	9000	1.14
20			P(1-2-B)	73	7400	1.20
21			P(1-2-1-C)	82	10400	1.28
22	VSM1	SA3	P(1-3-A)	88	10700	1.15
23			P(1-3-B)	83	6900	1.18
24			P(1-3-1-C)	96	14000	1.63
25	VSM5	SA1	P(5-1-2-C)	93	14100	1.69
26	VSM1	SA1	P(1-1-3-C)	89	15600	1.69
27	VSM1	SA1	P(1-1-4-C)	92	18700	1.67

Condition for pathway A: CuCl (10 mol%), solvent: DCM, temperature: 25 °C, base: DIPEA (2 equiv). The polymerization was carried out in the glovebox.
Condition for pathway B: CuTC (20 mol%) [reacted for 1 h], $Rh_2(OAc)_4$ (20 mol%) [reacted for another 5 h], solvent: $CHCl_3$, temperature: 60 °C. The polymerization was carried out in the glovebox.
Condition for pathway C: CuCl (10 mol%), solvent: DCM, temperature: 25 °C, base: DIPEA (2 equiv), Nu: 2.5 equiv.
[a]Polymerizations were conducted using **VSM1-6** and **SA1-3** as the monomers. [VSM] = [SA] = 0.2 M; polymerization time was 6 h.
[b]Polymers were precipitated in MeOH for three times and the yields were calculated after the solvent evaporation.
[c]M_n and $Đ$ were determined by GPC in DMF with PS standards.

$Rh_2(OAc)_4$ in pathway B, which would possibly interfere the Cu(I)-catalyzed polymerization. The electron-effect exhibited negligible influence on all the pathways by comparing the polymerization results using **VSM1** and **VSM2**, which was possibly due to the weak correlation between electronic effect and cycloaddition reaction. *Meta*-substituted VSM (**VSM4**) could also facilitate successful polymerizations across all the pathways albeit with reduced M_ns due to the steric hindrance effect. **VSM5** containing biphenyl groups could give the similar polymerization results in all the pathways. Since the pathway C involved **Nu** as the third component, another 3 amine-based Nus (**Nu2-4**) were furthermore expanded, yielding **P(5-1-2-C), P(1-1-3-C)** and **P(1-1-4-C)** (entries 25-27 in Table 1) in high yields (~90%) and M_ns (14,100 g/mol–18,700 g/mol). Thermal gravimetric analysis (TGA) results of four groups of polymers revealed that the polymers from all the pathways exhibited excellent thermal stability, with the $Td_{5\%}$ higher than 200 °C (Supplementary Fig. 105). The polymers prepared by pathway C owned notably higher $Td_{5\%}$ compared to those from pathway A or B, which was possibly due to the thermal stability of amidines compared to imines or imidates. **P(5-1-1-C)** with biphenyl group showed the best thermal stability, with the $Td_{5\%}$ up to 332.6°C. Differential scanning calorimetry (DSC) results indicated that the selected polymers were amorphous (Supplementary Fig. 106). Polymers obtained from **SA3** (**P(1-3-A), P(1-3-B)**, and **P(1-3-1-C)**) owned relatively lower Tg (99°C, 78°C, 74°C, respectively), which could be attributed to the **SA3**'s flexible chain. **P(5-1-1-C)** owned highest Tg up to 180°C because of the existence of rigid biphenyl group.

As a typical example, the chemical structures of **VSM1** and it is response three products **P(1-1-A), P(1-1-B)**, as well as **P(1-1-1-C)**, were carefully confirmed by ^{1}H-NMR spectra (Fig. 3A). The peak at δ 6.69 ppm representing the propargyl proton (peak a in **VSM1**) and the peak at δ 3.89 ppm (peak b in **VSM1**) representing the alkyne proton thoroughly disappeared in all the polymers, indicating the transformation of alkyne group. The proton resonance in -OCH_3 at δ 3.85 ppm (peak c in **VSM1**) completely vanished in the ^{1}H-NMR spectrum of **P(1-1-1-C)** while maintained in **P(1-1-A)** and **P(1-1-B)** (peak c' and c"), demonstrating the elimination of ester moiety in pathway C while migration in pathway A and B. Typical two alkene protons (peak e/d and h/i) appeared in **P(1-1-A)** and **P(1-1-1-C)**, while for **P(1-1-B)**, an alkene proton peak around δ 6.82 ppm and an imino proton peak at 7.67 ppm were viewed. ^{1}H-^{1}H COSY spectra of the model polymers also verified the assignment of alkene protons (Supplementary Figs. 1-3). To further determine the configuration of the alkenes in **P(1-1-A)** and **P(1-1-1-C)**, small molecule model compounds **M(10-4-A)** and **M(10-4-1-C)** were synthesized (Supplementary Figs. 4–5 & Supplementary Figs. 98–101). Basing on the coupling constants of two protons in alkenes, the structures could be verified to be *trans*-alkenes with excellent *E*-configuration stereoselectivity (J = 15.3 Hz for **M(10-4-A)** and J = 16.6 Hz for **M(10-4-1-C)**). By comparing the ^{1}H-NMR spectra of the small molecule model compounds and their corresponding polymers, the configurations of the alkenes in **P(1-1-A)** and **P(1-1-1-C)** were *trans*-alkenes as well. In pathway B, Rh(II)-catalyzed 1,2-ester migration would also afford *E*-alkenes, which was mainly controlled by the gauche strain reported by Li and us before[31–33]. Besides ^{1}H-NMR, matrix-assisted laser desorption/ionization time-of-flight (MALDI-TOF) was also utilized to analyze polymers' repeating units and the end groups. **P(1-1-A), P(2-1-B)**, and **P(1-1-1-C)** were selected as the typical polymers from pathways A, B, and C for MALDI-TOF analysis (Supplementary Figs. 6-8). However, only low m/z fragments could be observed because the unsaturated backbones were easy to fragile upon MALDI-TOF testing. Nonetheless, the results clearly indicated that all the polymers exhibited a set of correct peak spacing with the interval equal to the theoretical repeating unit value. In **P(1-1-A)**, m/z values equal to $[n\times778+Na]^+$ were clearly viewed (n = 1 to 5), indicating that **P(1-1-A)** was possibly a cyclic polymer without end-group (Supplementary Fig. 6). In **P(2-1-B)**, the m/z value of 1319.6 indicated the propargylic ester **VSM2** might serve as the terminal group in pathway B (Supplementary Fig. 7). Alkyne as the terminal group could be potentially utilized for the end-group functionalization via click chemistry[34]. The end-group analysis of pathway C was further discussed in the MCP section using **P(7-4-5-C)** as an example.

Since the polymers from pathway A and B owned exactly same repeating unit, MALDI-TOF results could not definitely determine their precise chemical structures. To in-depth demonstrate and differentiate the precise migrating position, both **P(1-1-A)** and **P(1-1-B)** were hydrolyzed for the further characterization by ^{1}H NMR and ^{13}C NMR (Fig. 3B, Supplementary Fig. 9). It was clearly observed that typical amide proton (-CON*H*-) appeared in **P(1-1-A)-H** around 12.41 ppm after hydrolysis (peak h in **P(1-1-A)-H**), indicating that the original structure was 1,3-migrating product. As for the 1,2-migrating product, typical benzyl protons (-CH_2-C_6H_4-) appeared around 3.8 ppm in **P(1-1-B)-H** (peak i in **P(1-1-B)-H**), indicating that the original structure was 1,2-migrating product. **P(5-1-A)** and **P(5-1-B)** were also successfully hydrolyzed to the corresponding amide and ketone, respectively

https://doi.org/10.1038/s41467-025-57619-7

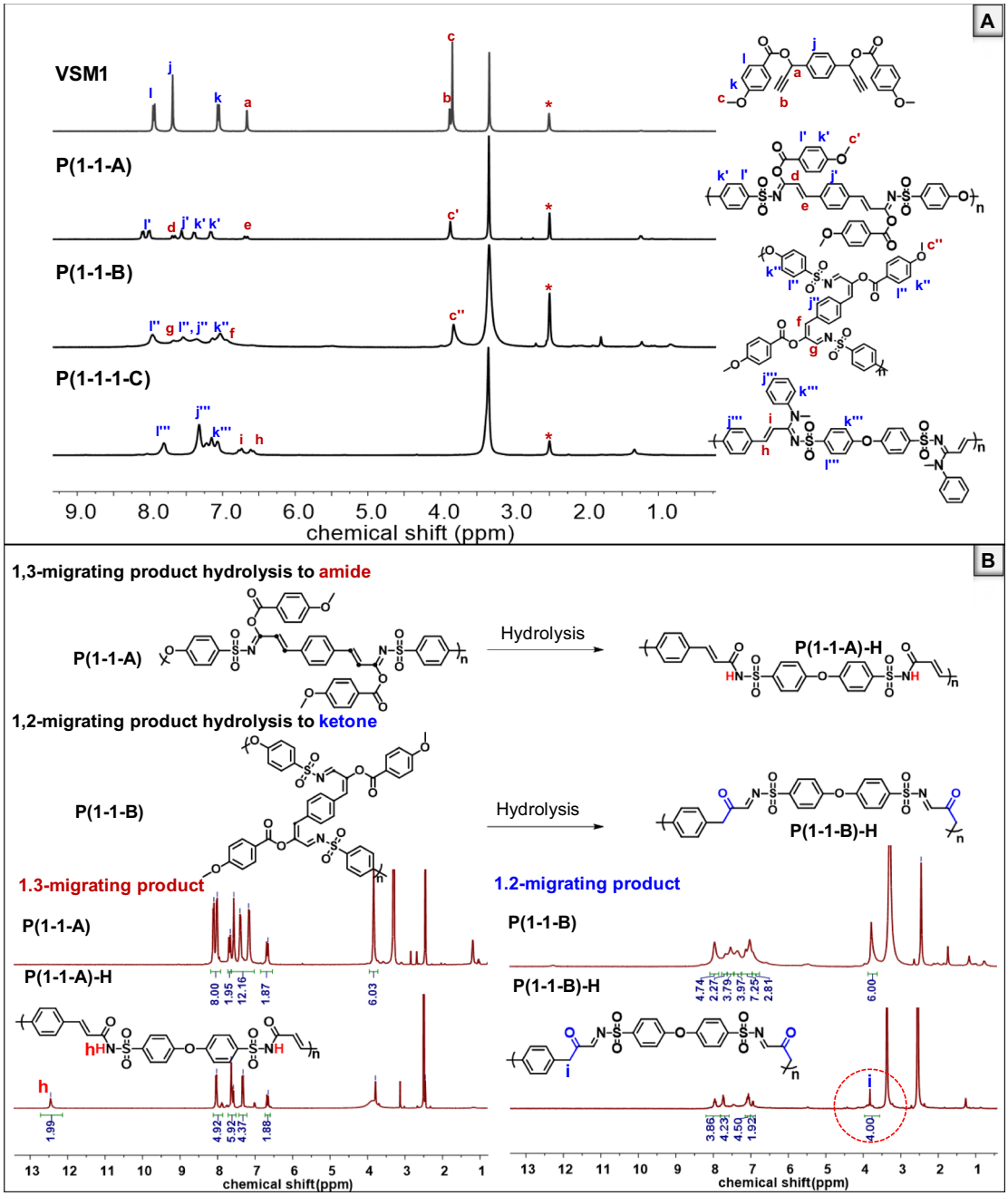

Fig. 3 | Structure characterization. A ^{1}H-NMR spectra of **VSM1, P(1-1-A), P(1-1-B)** and **P(1-1-1-C)**. The solvents were marked with asterisks (d_6-DMSO for **VSM1** and all the polymers). **B** Hydrolysis of **P(1-1-A)** and **P(1-1-B)** to **P(1-1-A)-H** and **P(1-1-B)-H**, respectively.

(Supplementary Fig. 10). The hydrolysis of other polymers in the library could be predicted.

Effect of ester leaving ability on the polymerization

Propargylic benzoates have been demonstrated with the capability of either migrating or leaving, which inspired us to furthermore investigate whether propargylic carbonate-bearing OBoc group could exhibit similar features. It was unexpected to find that both pathway A and pathway B failed because the leaving of -OBoc group occurred very fast (in 5 min) with the generation of messy products (Fig. 4A). Nevertheless, the MCP in pathway C underwent smoothly, affording **P(7-1-1-C)** with the same chemical structures of **P(1-1-1-C)** (Supplementary Figs. 76–77). When the benzoate group was changed to OBoc group, the ester would quickly leave since the leaving product for OBoc was CO_2 and $^tBuO^-$. It was interesting to find that **P(7-1-1-C)** owned higher M_ns (15800 g/mol) compared to **P(1-1-1-C)**, which could be attributed to rapid ester-leaving promoted polymerization reactivity (Fig. 4B, C). Related information would be discussed in detail in the mechanism section. Therefore, monomers bearing OBoc groups were furthermore explored as an expanded pathway C to prepare high M_n polyamidines.

Expanded pathway C using monomers bearing OBoc group for MCP

Since MCP involved three monomers, a flexible combination of di-OBoc monomers, *p*-toluenesulfonyl azide (TsN_3), and Nus bearing diamines/diols could be designed as a variant of pathway C (expanded pathway C in Fig. 5A). Except the commercially available monomers, all monomers were systematically synthesized and characterized

https://doi.org/10.1038/s41467-025-57619-7

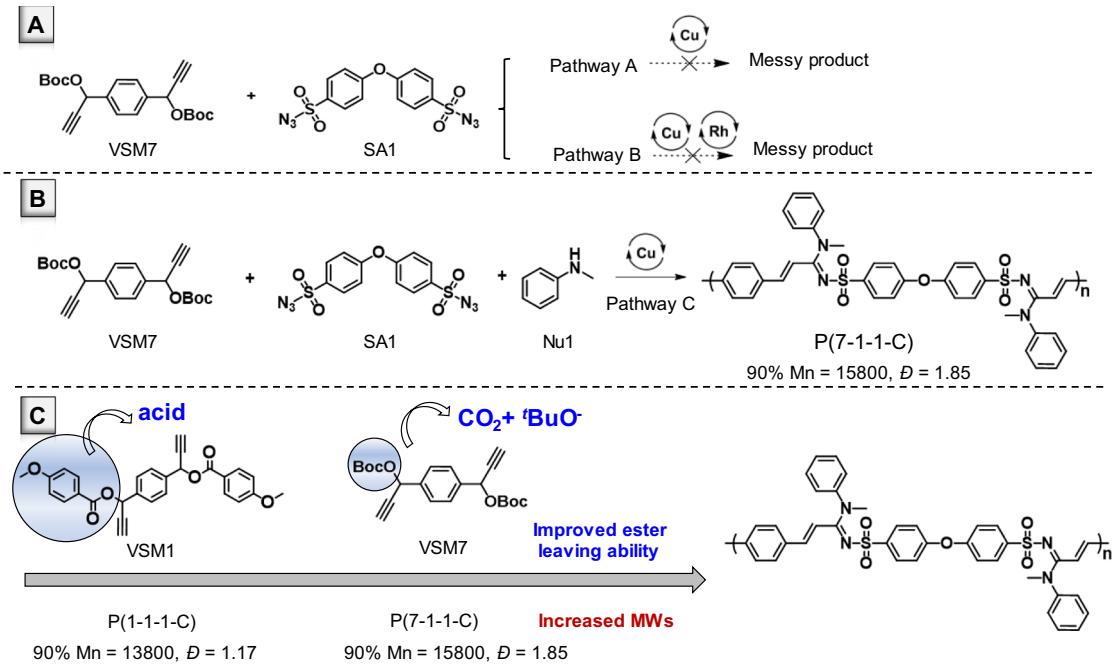

Fig. 4 | Comparison of different VSM monomers. A Polymerization of **VSM7** and **SA1** under pathway A and pathway B. **B** MCP of **VSM7, SA1,** and **Nu1** under pathway C. **C** Comparison of polymerization results using different VSM monomers.

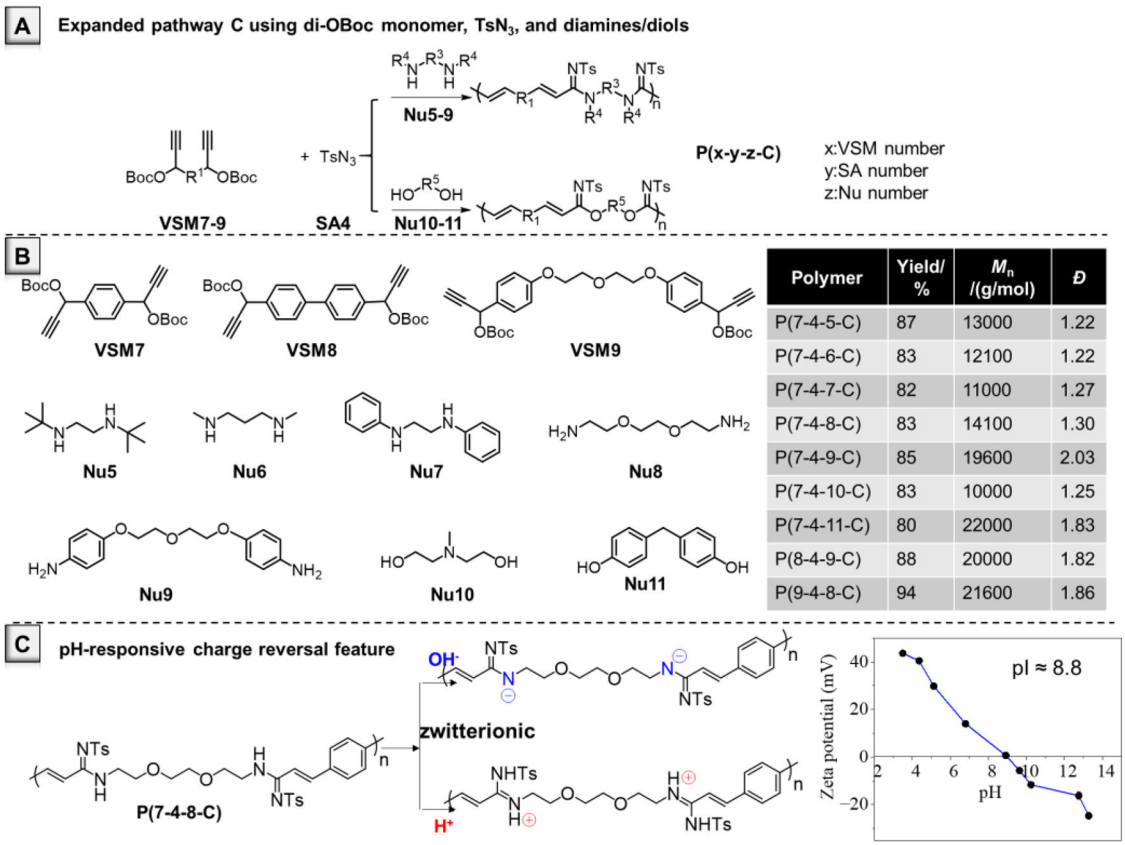

Polymer	Yield/ %	M_n /(g/mol)	Đ
P(7-4-5-C)	87	13000	1.22
P(7-4-6-C)	83	12100	1.22
P(7-4-7-C)	82	11000	1.27
P(7-4-8-C)	83	14100	1.30
P(7-4-9-C)	85	19600	2.03
P(7-4-10-C)	83	10000	1.25
P(7-4-11-C)	80	22000	1.83
P(8-4-9-C)	88	20000	1.82
P(9-4-8-C)	94	21600	1.86

Fig. 5 | Multicomponent polymerization. A Expanded pathway C using **VSM7-9, SA4**, and **Nu5-11**. **B** Monomer substrate and polymerization results. **C** Charge-reversal properties of zwitterionic **P(7-4-8-C)** as demonstrated by the zeta potentials under different pH values.

(monomer ^{1}H NMR: Supplementary Figs. 25–34; polymer ^{1}H NMR: Supplementary Figs. 78–91; GPC: Supplementary Fig. 104). The MCP conditions including the solvent, temperature, catalysts, monomer concentrations, loading ratios, bases, and polymerization time were optimized using **VSM7, SA4**, and **Nu5** as the model monomers towards **P(7-4-5-C)**. (Tables S1–S8, the detailed condition optimization results were discussed in the supporting information). The chemical structures of **P(7-4-5-C)** were determined by ^{1}H-NMR and ^{13}C-NMR

(Supplementary Fig. 15). MALDI-TOF was used to analyze the repeating unit and end-group of the resulting polymer (Supplementary Fig. 15). The theoretical molecular weight of **P(7-4-5-C)**'s repeating unit was 660.3 g/mol, which could be clearly observed in MALDI-TOF results with a series of peaks (Supplementary Fig. 15). Two possible end-groups terminated by amine or Cu-allenylidene could also be found, indicating that the removal of OBoc group occurred during the polymerization. Under the optimized MCP conditions, 9 polymers could be successfully obtained in high yields (80%-94%) with desired M_ns (10,000 g/mol−22,000 g/mol) (Fig. 5B, Supplementary Figs. 78–91). All the polymers owned excellent solubility in polar solvents like DMSO and DMF (Supplementary Table 10). Aliphatic secondary amine could provide polymers (**P(7-4-5-C)** and **P(7-4-6-C)**) with slightly higher M_ns compared to aromatic secondary amine (**P(7-4-7-C)**), which might be due to the stronger basicity and nucleophilicity. Because of the steric hindrance effect, primary amine outperformed secondary amine, and aromatic primary amine with multiple ester groups exhibited M_n up to 19,600 g/mol (**P(7-4-9-C)**). Diols could also serve as the nucleophiles to successfully facilitate MCP, affording polymers with highest M_ns up to 22,000 g/mol (**P(7-4-11-C)**). It was delighted to find that di-OBoc monomers bearing biphenyl groups or multiple ether groups could generate two polymers with the M_n higher than 20,000 g/mol (**P(8-4-9-C)** and **P(9-4-8-C)**), indicating the advantages of OBoc group with excellent leaving ability in producing high M_n polyamidines.

Amidine, as a typical base, can be protonated to be positive charge at acidic conditions. However, for the *N*-sulfonyl amidine, it exhibits weak acidity due to the existence of electro-withdrawing sulfonyl group. In this work, vinyl group could be spontaneously generated from above polymerization, which can be predicted with the ability to achieve the functionalization via thiol-ene click reaction[35]. Moreover, the introduction of vinyl group could also enrich the applications for the nitrogen-containing polymers due to the extended π-conjugated system. Taking **P(7-4-8-C)** as an example, its pH-responsive charge-reverse property was carefully studied in Fig. 5C. Based on the zeta potential results, it could be clearly viewed that **P(7-4-8-C)** can be de-protonated and showed negative charges (−20 mV) under basic conditions, which was in accordance with the previously reported poly(*N*-sulfonyl amidine) by our group[36,37]. However, the previously reported poly(*N*-sulfonyl amidine) without the conjugated vinyl group could only show neutral charge even the pH value was lower than 2. It was interesting to find that **P(7-4-8-C)** bearing vinyl sulfonyl amidine could also be protonated to positive charge (+40 mV) when the pH value decreased. The unique zwitterionic properties for the polyamidine could be attributed to the synergic effect of both the electron-withdrawing sulfonyl group and the conjugated vinyl benzyl group. The isoelectric point (pI) of **P(7-4-8-C)** was calculated to be 8.8. Obvious precipitates could be observed around the pI value while clear nanoparticle solutions could be recovered when tuning the pH values, indicating charge-reversal ability. Similarly, the pH-responsive charge reversal ability of vinyl sulfonyl amidine polymer was also verified by **P(9-4-8-C)** (Supplementary Fig. 16). Such observations enrich the applications of the traditional amidines as bases and the recently reported *N*-sulfonyl amidine as acids. The zwitterionic properties of poly(vinyl-*N*-sulfonyl amidine) could be potentially utilized for the preparation of charge-reversal materials in the smart trigger-responsive fields.

Mechanism study

To probe the mechanism of the polymerization, we followed the conversion of **SA1** to polymers (in different pathways) over time by ^{1}H NMR and GPC, respectively (Supplementary Fig. 11). The monomer conversion rate at different time points was determined by the in-situ ^{1}H NMR spectra (Supplementary Figs. 12–14), and the corresponding M_n was based on the GPC results. All the pathways exhibited step-growth polymerization mechanism. Then, a series of control experiments were performed. For pathway A, the [3,3]-sigmatropic rearrangement mechanism could be demonstrated by the in-situ ^{1}H-NMR spectra tracking the transformation of **VSM1** and **SA1** under Cu(I) catalysis. As shown in Supplementary Fig. 92, trace amount of *p*-anisic acid has been detected during the polymerization. Such phenomenon indicated the pathway A did not undergo the ester leaving followed by the acid addition mechanism. To explore the 1,2-migrating mechanism, the polymerization of **VSM1** and **SA1** was performed by a two-step method. Under the CuTC catalysis, **P(1-1-triazole)** could be obtained in 1 h and isolated with M_n of 8400 g/mol in 93% yield (eq.1 in Fig. 6, Supplementary Fig. 93). Upon the addition of $Rh_2(OAc)_4$ to **P(1-1-triazole), P(1-1-B)** could also be obtained without the dramatic change of yield and M_n (eq. 2 in Fig. 6, Supplementary Fig. 94). Such results indicated that the 1,2-migrating mechanism involved the formation of stable sulfonyl triazole, followed by the Rh(II)-mediated ring-open and ester migrating. Upon the addition of **Nu1** to **P(1-1-triazole), P(1-1-1-C)** was failed to obtain, meaning that the formation of polyamidine in pathway C did not go through the sulfonyl triazole intermediate (eq. 3 in Fig. 6). The case involving OBoc group also showed similar results with the successful preparation of OBoc-sulfonyl triazole from **VSM7** and **SA4** by CuTC, while failure to get **P(7-4-5-C)** with the addition of **Nu5** (eq. 4 and 5 in Fig. 6, Supplementary Figs. 95–96). The transformation of **VSM1, SA1**, and **Nu1** were tracked using in-situ ^{1}H-NMR under the pathway C conditions (Supplementary Fig. 97). Obvious carboxyl acid peaks were viewed from the in-situ ^{1}H-NMR spectrum during the polymerization, indicating the Nu induced ester leaving mechanism.

Based on the polymer structures, kinetic studies, control experiments, and relevant literatures, a tentative mechanistic picture for propargylic esters promoting polymerization was proposed in Fig. 7. In pathway A, direct [3 + 2] cycloaddition reaction of VSM and SA occurred fast to form *di*-triazole intermediate **A**. Then, in the presence of base, Cu(I)-assisted rearrangement occurred with extrusion of N_2 to afford *di*-ketenimine **B**. Due to the strong electrophile of ketenimine which might also coordinate with the π-acidic copper in the system, the pivotal 1,3-migrating (also as a type of [3,3]-sigmatropic rearrangement) of ester would exclusively perform. If the rhodium(II) was added as co-catalyst, α-imino rhodium-carbene intermediate **C** would be unexpectedly generated instead of ketenimine by the extrusion of N_2. Then, due to the strong electrophile of transition metal-carbene, the essential 1,2-migrating (also as a type of [2,3]-sigmatropic rearrangement) of ester would exclusively conduct in pathway B.

As for pathway C involving ester leaving, the polymerization could possibly follow two mechanisms as indicated by pathway C1 and pathway C2. Propargylic benzoates could possibly undergo pathway C1 since the cycloaddition happened prior to the ester leaving. After the formation of *di*-ketenimine **B**, the Nu would attack **B** to promote the ester leaving. When the ester was changed to OBoc group, it would quickly leave before the cycloaddition since the leaving product for OBoc was CO_2 and $^tBuO^-$. In the presence of base, propargylic ester initially coordinated with copper(I) to form copper acetylide, which promoted the ester leaving by an S_N1 mechanism to generate cationic intermediate **D** or copper-allenylidene complex **D'** as a resonance structure (The intermediate after the removal of ester was trapped by GC-MS (gas chromatography-mass spectrometry) with HRMS (m/z = 115.0542) as shown in Supplementary Fig. 17). Then the [3 + 2] cycloaddition reaction of TsN_3 and Cu-allenylidene (**D'**) occurred to form the unstable intermediate **E** which rapidly converted to carbene intermediate **F** by the removal of copper catalyst. Then, a carbene-assisted rearrangement occurred with extrusion of N_2 to afford *di*-alkylidene ketenimine **G**, which was further trapped by GC-MS with HRMS (m/z = 283.0658) as shown in Supplementary Fig. 18. Finally, the additional nucleophile could quickly attack alkylidene ketenimine **G** by desired nucleophilic addition. The mechanism difference between pathway C1 and C2 also explained the

https://doi.org/10.1038/s41467-025-57619-7

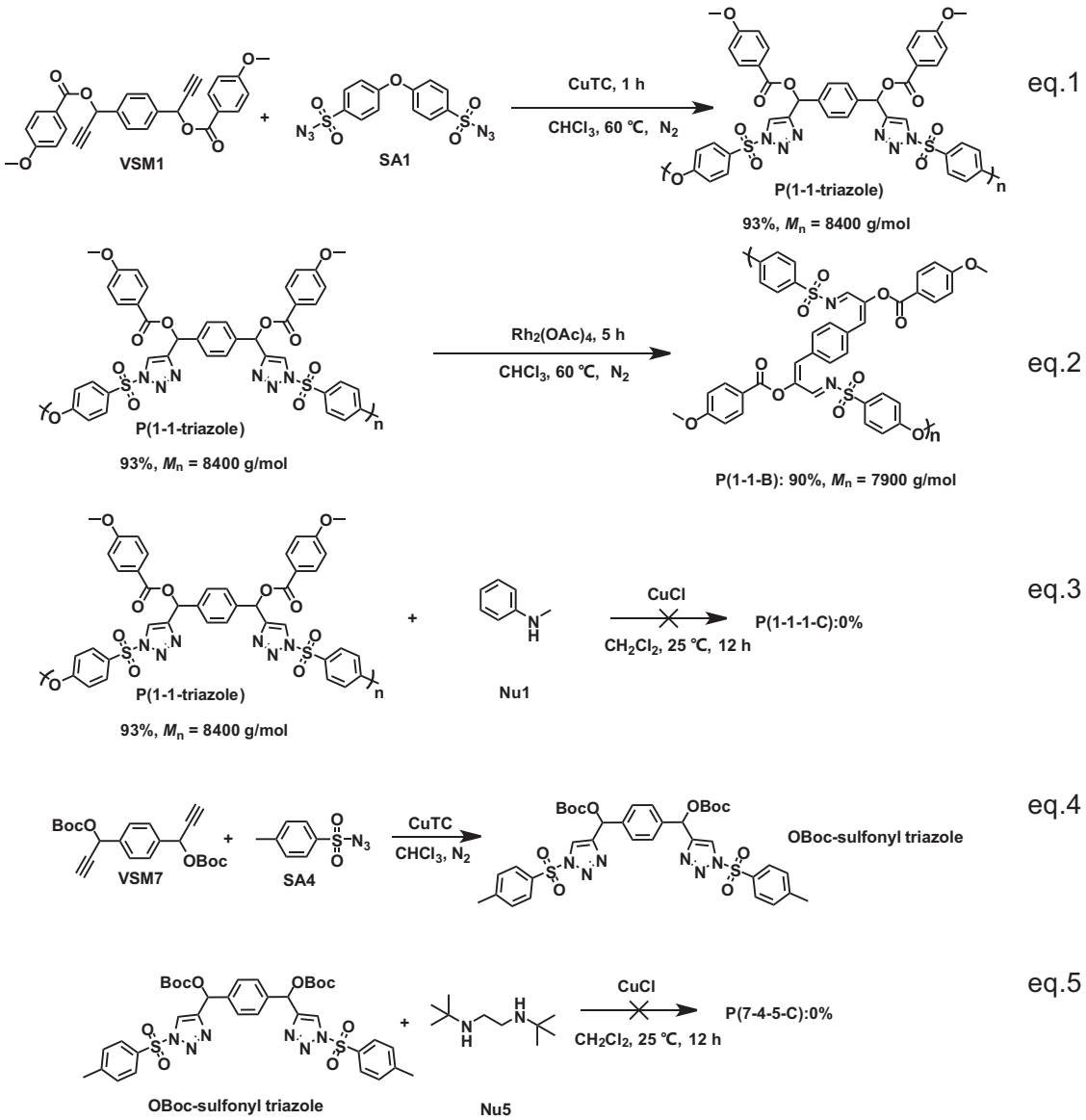

Fig. 6 | Mechanism experiments. Control experiments for the polymerization mechanism study.

improved M_n for monomers bearing OBoc groups. From the reactivity aspect, all the polymerizations underwent the cycloaddition process, which was also the key step in determining the M_ns. In most of the cases, the cycloaddition occurred between azide and alkyne in propargylic ester. While in pathway C2, Cu-allenylidene (**D'**) (the leaving of ester could induce the generation of Cu-allenylidene **D'**) instead of Cu-alkyne participated in the cycloaddition, thereby with improved reactivity.

In this work, propargylic ester was designed as the VSM to induce tunable polymerizations with the facile preparation of structure-diverse polymers. By controlling the migrating or leaving property of the esters, polyimidates, polyimines, and polyamidines could be obtained under different conditions. The mechanism study verified that the ketenimine, imine, and alkylidene ketenimine intermediates were involved in different pathways. By carefully tuning the polymerization conditions, triple number of polymers could be obtained from identical monomer combinations. The ester-leaving induced MCPs have also been systemically expanded to a library of polymers bearing vinyl groups conjugated to sulfonylamidines. Such features bestowed the polymers with zwitterionic properties and pH-responsive charge-reversal functions. The design of VSM provided new insights into the precise control of polymer structures by selective transformation of specific monomers. Such strategy would also offer the guidance in rapidly and flexibly constructing structure-diverse polymer library.

Methods

Polymerization method for pathway A

VSM1 (0.5 mmol, 227 mg, 1 equiv), **SA1** (0.5 mmol, 190 mg, 1 equiv) and DIPEA (1 mmol, 170 μL, 2 equiv) were dissolved in anhydrous DCM (2.5 mL) in the glovebox. Then CuCl (0.05 mmol, 5.0 mg, 0.1 equiv) was added, and immediately bubbles appeared in this reaction system. The mixture was stirred for 6 h at room temperature, the product was precipitated using MeOH and collected by centrifugation. The polymer **P(1-1-A)** was dried under vacuum.

Polymerization method for pathway B

Polymerization pathway B was performed in a glove box as mentioned below to prepare polyimine. **VSM1** and **SA1** were used as a typical example. **VSM1** (0.2 mmol, 90.8 mg, 1 equiv) and **SA1** (0.2 mmol, 76 mg, 1 equiv) were dissolved in anhydrous $CHCl_3$ (1 mL) in a 5 mL glass vial. Then CuTC (0.04 mmol, 7.6 mg, 0.2 equiv) was added and

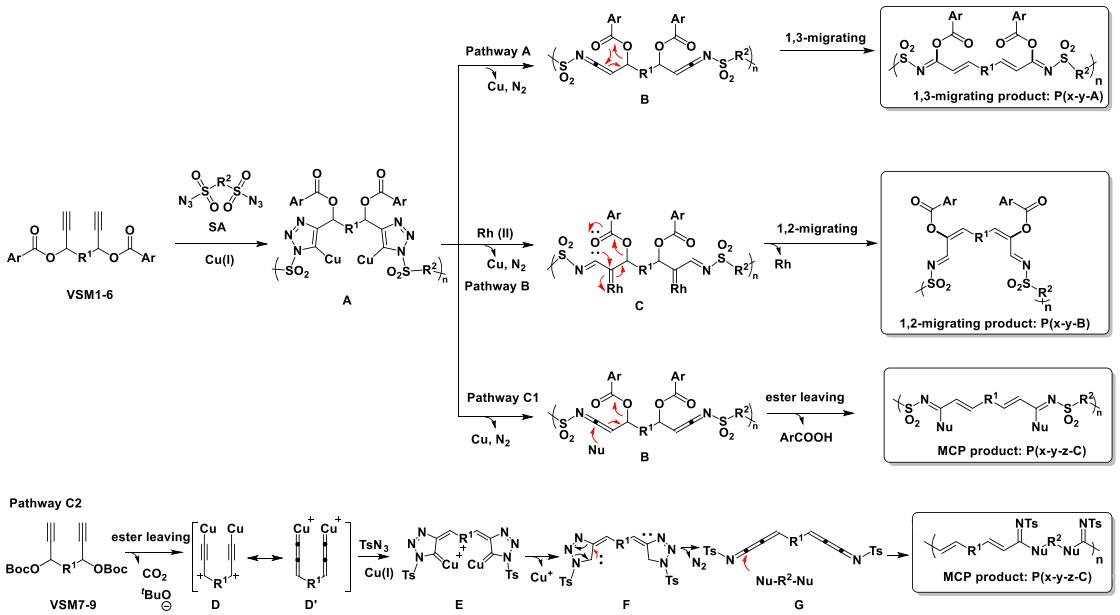

Fig. 7 | Polymerization mechanisms. Proposed mechanism for different polymerization pathways.

stirred for 1 h at 60°C. Subsequently, $Rh_2(OAc)_4$ (0.04 mmol, 17.6 mg, 0.2 equiv) was added and stirred for 5 h at the same temperature. The product was precipitated using MeOH and collected by centrifugation. The polymer **P(1-1-B)** was dried under vacuum.

Polymerization method for pathway C

The polymerization pathway C was performed in air as mentioned below to prepare polyamidine. **VSM1, SA1**, and **Nu1** were used as a typical example. **VSM1** (0.5 mmol, 227 mg, 1 equiv), **SA1** (0.5 mmol, 190 mg, 1 equiv), **Nu1** (1.25 mmol, 135 µL, 2.5 equiv), and DIPEA (1 mmol, 170 µL, 2 equiv) were dissolved in anhydrous DCM (2.5 mL) in a 10 mL glass vial. Then CuCl (0.05 mmol, 5 mg, 0.1 equiv) was added, and immediately bubbles appeared in this reaction system. The mixture was stirred for 6 h at room temperature, the product was precipitated using MeOH and collected by centrifugation. The polymer **P(1-1-1-C)** was dried under vacuum.

Data availability

All data generated and analyzed in this paper are available in the Supplementary Information. Experimental procedures, characterization of structure, and zeta potentials are available in the Supplementary information. All data are available from the corresponding author upon request.

References

1. Shen, W. B. et al. Divergent synthesis of *N*-heterocycles via controllable cyclization of azido-diynes catalyzed by copper and gold. *Nat. Commun.* **8**, 1748 (2017).
2. Li, L., Chen, Z., Zhang, X. W. & Jia, Y. X. Divergent strategy in natural product total synthesis. *Chem. Rev.* **118**, 3752–3832 (2018).
3. Chintawar, C. C., Yadav, A. K., Kumar, A., Sancheti, S. P. & Patil, N. T. Divergent gold catalysis: unlocking molecular diversity through catalyst control. *Chem. Rev.* **121**, 8478–8558 (2021).
4. Zhang, W. B. et al. Molecular nanoparticles are unique elements for macromolecular science: from "nanoatoms" to giant molecules. *Macromolecules* **47**, 1221–1239 (2014).
5. Kreye, O., Tóth, T. & Meier, M. A. R. Introducing multicomponent reactions to polymer science: passerini reactions of renewable monomers. *J. Am. Chem. Soc.* **133**, 1790–1792 (2011).
6. Xue, H. D. et al. Multicomponent combinatorial polymerization via the biginelli reaction. *J. Am. Chem. Soc.* **138**, 8690–8693 (2016).
7. Corey, E. J. General methods for the construction of complex molecules. *Pure Appl. Chem.* **14**, 19–38 (1967).
8. Desiraju, G. R. Supramolecular synthons in crystal engineering-a new organic synthesis. *Angew. Chem. -Int. Edit.* **34**, 2311–2327 (1995).
9. Wang, X. N. et al. Ynamides in ring forming transformations. *Accounts Chem. Res.* **47**, 560–578 (2014).
10. Lundberg, P., Hawker, C. J., Hult, A. & Malkoch, M. Click assisted one-pot multi-step reactions in polymer science: accelerated synthetic protocols. *Macromol. Rapid Commun.* **29**, 998–1015 (2008).
11. Lee, I. H., Bang, K. T., Yang, H. S. & Choi, T. L. Recent advances in diversity-oriented polymerization using Cu-catalyzed multicomponent reactions. *Macromol. Rapid Commun.* **43**, 2100642 (2022).
12. Lu, P. & Wang, Y. The thriving chemistry of ketenimines. *Chem. Soc. Rev.* **41**, 5687–5705 (2012).
13. Kim, S. H., Park, S. H., Choi, J. H. & Chang, S. Sulfonyl and phosphoryl azides: going further beyond the click realm of alkyl and aryl azides. *Chem. -Asian J.* **6**, 2618–2634 (2011).
14. Duan, X. L. et al. Copper-catalyzed *Z*-selective synthesis of acrylamides and polyacrylamides via alkylidene ketenimines. *Nat. Commun.* **13**, 4362 (2022).
15. Ma, T. Q. et al. Single-crystal x-ray diffraction structures of covalent organic frameworks. *Science* **361**, 48–52 (2018).
16. Xu, W. T. et al. A metal-organic framework of organic vertices and polyoxometalate linkers as a solid-state electrolyte. *J. Am. Chem. Soc.* **141**, 17522–17526 (2019).
17. Lin, S. et al. Covalent organic frameworks comprising cobalt porphyrins for catalytic CO_2 reduction in water. *Science* **349**, 1208–1213 (2015).
18. Lee, I. H., Kim, H. & Choi, T. L. Cu-Catalyzed multicomponent polymerization to synthesize a library of poly(*N*-sulfonylamidines). *J. Am. Chem. Soc.* **135**, 3760–3763 (2013).
19. Kim, H., Bang, K. T., Choi, I., Lee, J. K. & Choi, T. L. Diversity-oriented polymerization: one-shot synthesis of library of graft and dendronized polymers by Cu-catalyzed multicomponent polymerization. *J. Am. Chem. Soc.* **138**, 8612–8622 (2016).

20. Xu, L., Hu, R. R. & Tang, B. Z. Room temperature multicomponent polymerizations of alkynes, sulfonyl azides, and iminophosphorane toward heteroatom-rich multifunctional poly(phosphorus amidine)s. *Macromolecule* **50**, 6043 (2017).
21. Xu, L., Zhou, T., Liao, M., Hu, R. R. & Tang, B. Z. Multicomponent polymerizations of alkynes, sulfonyl azides, and 2-hydroxybenzonitrile/2-aminobenzonitrile toward multifunctional iminocoumarin/quinoline-containing poly(*N*-sulfonylimine)s. *ACS Macro Lett* **8**, 101–106 (2019).
22. He, J. N., Zheng, N., Li, M., Zheng, Y. B. & Song, W. Z. Cu-Catalyzed four-component polymerization of alkynes, sulfonyl azides, nucleophiles and electrophiles. *Polym. Chem*. **12**, 4347–4358 (2021).
23. Sun, H. L. et al. Synthesis of polydiynes via an unexpected dimerization/polymerization sequence of C3 propargylic electrophiles. *J. Am. Chem. Soc.* **144**, 8807–8817 (2022).
24. Wang, Z. Y. & Zhu, R. Conjugated [5]cumulene polymers enabled by condensation polymerization of propargylic electrophiles. *J. Am. Chem. Soc.* **145**, 23755–23763 (2023).
25. Wang, Z. L. & Zhu, R. Regioselective condensation polymerization of propargylic electrophiles enabled by catalytic element-cupration. *J. Am. Chem. Soc.* **146**, 19377–19385 (2024).
26. Shu, X. Z., Shu, D. X., Schienebeck, C. M. & Tang, W. P. Rhodium-catalyzed acyloxy migration of propargylic esters in cycloadditions, inspiration from the recent "gold rush. *Chem. Soc. Rev.* **41**, 7698–7711 (2012).
27. Xu, Z. F. et al. Synthesis of cyclopropanes via 1,3-migration of acyloxy groups triggered by formation of α-imino rhodium carbenes. *Org. Lett.* **22**, 5163–5169 (2020).
28. Raushel, J. & Fokin, V. V. Efficient synthesis of 1-sulfonyl-1,2,3-triazoles. *Org. Lett.* **12**, 4952–4955 (2010).
29. Wang, Y. & Zhang, Z. Multicomponent synthesis of imidazole-based cross-conjugated polymers via bimetallic Cu(I)/Rh(II) relay catalysis. *Macromolecules* **55**, 5422–5429 (2022).
30. Wang, Y. et al. Bimetallic Cu(I)/Rh(II) relay catalysis for multicomponent polymerization through carbene intermediates. *Macromolecules* **55**, 643–651 (2022).
31. Dai, H., Yu, S., Cheng, W., Xu, Z. & Li, C. Rhodium-catalyzed synthesis of 1,2-dihydropyridine by a tandem reaction of 4-(1-acetoxyallyl)-1-sulfonyl-1,2,3-triazole. *Chem. Commun.* **53**, 6417–6420 (2017).
32. Zheng, N. & Song, W. Synthesis and application of 1,2,3-triazole allyl acetates: expedient access to pyridine derivatives. *Heterocycles* **94**, 1289–1295 (2017).
33. Chen, J., Chen, Z., Yu, M., Xu, Z., Li, C. Rhodium-catalyzed synthesis of polycyclic Spiroindolines via intramolecular 1,2-acyloxy migration-cyclization cascade. *Eur. J. Org. Chem*. e202400944 (2024). https://doi.org/10.1002/ejoc.202400944.
34. Zaccaria, C. et al. Biocompatible graft copolymers from bacterial poly(γ-glutamic acid) and poly(lactic acid). *Polym. Chem.* **12**, 3784–3793 (2021).
35. Fornaciari, C., Invernizzi, F., Galbiati, A. & Pasini, D. Solvent-free thiol-ene/-yne click reactions for the synthesis of alkoxysilyl telechelic poly(propylene oxide)s. *React. Funct. Polym.* **200**, 105939 (2024).
36. Xu, X., Ma, J. J., Wang, A. G. & Zheng, N. *N*-Sulfonyl amidine polypeptides: new polymeric biomaterials with conformation transition responsive to tumor acidity. *Chem. Sci.* **15**, 1769–1781 (2024).
37. Tian, E. L., Li, M., Song, W. Z. & Zheng, N. Catalyst-free multicomponent polymerization of sulfonyl azide, aldehyde and cyclic amino acids toward zwitterionic and amphiphilic poly(*N*-sulfonyl amidine) as nanocatalyst precursors. *Sci. China-Chem.* **65**, 1798–1806 (2022).

Acknowledgements

This work was supported by grants from the National Natural Science Foundation of China (22375027) (to N.Z.), and the Fundamental Research Funds for the Central Universities (DUT23YG133 to N.Z., DUT24ZD114 to W.S.). The authors acknowledge the assistance of DUT Instrumental Analysis Center.

Author contributions

N.Z. designed the study. H.H., X.D., M.L., H.S., and G.W. performed the experiments. H.H., X.D., and M.L. analyzed the data. N.Z., H.H., X.D. W.S. and M.L. wrote the manuscript. All authors discussed the results and commented on the manuscript.

Competing interests

The authors declare no competing interests.

Additional information

Supplementary information The online version contains supplementary material available at https://doi.org/10.1038/s41467-025-57619-7.

Correspondence and requests for materials should be addressed to Nan Zheng.

Peer review information *Nature Communications* thanks Jeffrey Foster and the other, anonymous, reviewer(s) for their contribution to the peer review of this work. A peer review file is available.